# BRDF Normalization of Hyperspectral Image Data

H. Peter White[1], Lixin Sun[2], Catherine M. Champagne[3], Karl Staenz[1], Sylvain G. Leblanc[1]

1) Canada Centre for Remote Sensing, Natural Resources Canada, 588 Booth Street, Ottawa, Ontario, Canada, K1A 0Y7
2) Dendron Resource Surveys Inc., Ottawa, K1Z 5L9
3) MIR Télédétection Inc., Québec, J4K 1A3

**Abstract – Monitoring vegetative areas with airborne hyperspectral sensors is being more frequently used to relate at-canopy spectral reflectance to canopy condition. Increased application of these techniques is expected with the advent of space borne hyperspectral systems (such as EO-1 Hyperion and CHRIS-PROBA). These studies are often limited by the non-Lambertian nature of vegetation reflectance, the well known bidirectional reflectance distribution function (BRDF), where varying solar and viewing geometry can result in significant variations in the observed remotely sensed signal due to canopy architectural properties. This is often noted as an increased brightening of the observed signal as the scattering angle between the sun and sensor decreases. This is also true when attempting to compare images from different sensors, or from the same sensor taken at different times. Various studies have examined the sensitivity of broadband and hyperspectral vegetation indices (VI) to BRDF. These studies often conclude that the choice of VI should be based on the solar/viewing geometry and vegetation specific to the image acquisition. No individual VI appears immune to the BRDF effect.**

**Rather than attempt to define a technique with little sensitivity to view/solar geometry, the non-Lambertian reflectance characteristics can be used to normalize imagery to one view/solar geometry. Assuming consistent mean leaf and background reflectance, inversion of a semi-empirical model can be used to determine BRDF coefficients, which can then be applied to normalize the imagery to a specific viewing/solar geometry. If the model has coefficients that directly relate to canopy properties, then this process can also provide information directly relating canopy architectural and biophysical properties to the remotely sensed signals. One such model, FLAIR, has been successfully used to investigate canopy characteristics from broadband imagery. Application of this model to hyperspectral imagery of an agricultural area is being pursued, examining the usefulness of normalizing the BRDF before relating spectral reflectance to biophysical characteristics.**

## I. Introduction

Interest in the application of hyperspectral remote sensing has increased over the past two decades, leading to a variety of studies which examine relationships between this data and various environmentally significant parameters. High resolution spectral reflectance of vegetative surfaces provide a variety of spectral features which can be identified. Several studies focus on the amplitude of absorption features as a method of identifying canopy condition. Vegetation indices (VI's), calculated as linear combinations of two (or more) spectral reflectance factors, have been found to correlate with canopy cover [1][2], effective leaf area index (*eLAI*) [3][4], relative water content (RWC) [5][6], and canopy chlorophyll density (CCD) [1][4]. Surface spectral reflectance has also been used to identify and separate component fractions contributing to the observed canopy reflectance [7]. It has been shown however that such applications are sensitive to background reflectance (soil, residue, ground cover) [8][4] and view/illumination geometry (the bidirectional reflectance distribution function, or BRDF effect) [9][10].

To further the development of these studies, the influence of the background reflectance and BRDF on remotely sensed signals needs to be identified. One commonly applied method is to develop and apply a semi-empirical canopy radiative transfer model, inverting the model to input observed bidirectional reflectance factors (BRF's) to determine model coefficients. These can be used to identify the significance of the background reflectance, and to normalize observed BRF's to a common view/illumination geometry. [10][11][12]

FLAIR (**F**our-Scale **L**inear Model for **A**n**I**sotropic **R**eflectance) has been successfully tested with broadband spectral reflectance of boreal forests [11][14]. This allows observed BRF's to be normalized to a common view/illumination geometry for determining broadband spectral VI's. This model has been modified for application to hyperspectral data, allowing inversion of high resolution spectral reflectance for BRDF normalization. Testing of this model has been performed with data collected over agricultural regions of southwest Ontario, during the summer of 1999, taken with the Probe-1 hyperspectral sensor.

## II. Data Acquisition

An agricultural study area near Clinton, Ontario (43° 40' N; 81° 30' W) was identified and used as part of a study examining the potential development of hyperspectral remote sensing data products useful for precision farming. The area is mainly corn, bean, and small grain (wheat and barley) crops. A few mixed deciduous forested areas also exist.

Detailed ground surveys of specific fields, including canopy cover, reflectance, and *eLAI*, were taken during this study [1][3]. Airborne Probe-1 hyperspectral imagery was acquired on 7-July, with mid- and late-morning passes. The imagery consists of 128 spectral bands ranging from 430 nm to 2500 nm, with a pixel spatial resolution of 5 m × 5 m. Hyperspectral surface reflectance imagery was produced using the Imaging Spectrometer Data Analysis System (ISDAS) [13] developed at Natural Resources Canada – Canada Centre for Remote Sensing.

## III. Model Inversion Development

The FLAIR model was initially developed for inversion of broadband reflectance imagery [10][11]. In short, this model relates observed BRF to the sum of four component mean reflectance factors (for more detail, see [10]), expressed as:

$$BRF = R_{zt} \times k_{zt} + R_{zg} \times k_{zg} + R_t \times k_t + R_g \times k_g \qquad (1)$$

where $R_x$ are the four scene component mean reflectance factors defined as the ratio of nadir reflected radiance from the scene component to nadir reflected radiance which would be reflected by a 100% reflecting Lambertian panel located at the top of the canopy, above the target component. The four scene components are shaded overstorey (*zt*); shaded background (*zg*); directly sunlit overstorey (*t*); and directly sunlit background (*g*). $k_j$ are the viewed scene component proportions, functions of view/solar geometry and *eLAI*.

Inversion was performed over a range of *eLAI*, using a modified simplex method [10], with the the optimal result identified based on a comparison of the observed and derived BRF's (using root mean square error and/or correlation coefficient). Defined by this model, shaded and sunlit reflectance factors are independent values, which is not true. These values are related by having user determined multi-scattering limits ($MS_t$ and $MS_g$, defined as the ratio of shaded to sunlit reflectance factors for the overstorey and background respectively) where the multi-scattering factors have to be similar (one within a set percentage of the other).

For application to hyperspectral data, the model required additional development: i) multiple spectral bands had to be inverted concurrently; and ii) shaded reflectance factors had to be more closely linked to sunlit reflectance factors. The model was developed as a tool in ISDAS to allow for ease of interaction with hyperspectral data cubes.

The ability to invert FLAIR with multiple bands was developed by expanding (1) for *n* bands, thus providing 4*n*+1 model coefficients ($R_{x_n}$,*eLAI*). These coefficients are related in the inversion such that all $k_j$ for bands $m \neq n$ are zero. Thus only the four component reflectance factors for a specific band are contributing to the BRF's of that band.

$$BRF_n = R_{zt_n} \times k_{zt} + R_{zg_n} \times k_{zg} + R_{t_n} \times k_t + R_{g_n} \times k_g \qquad (2)$$

The option of relating $R_{x_n}$ between bands was also considered, for example setting the near infrared band overstorey reflectance factors to be greater than the red band overstorey reflectance factors. This would increase the number of constraints by $n^2$, increasing computational time. As FLAIR automatically restricts $R_x$ to between 0 and 1, and $k_j$ between 0 and 1, and as the sum of the four products are limited by the observed BRF's for each band, additionally constraining one band relative to another was found unnecessary. Thus the only factors relating reflectance between bands are canopy *eLAI* and view/solar geometry, inputs to the four kernels.

Multi-scattering factors were initially limited, requiring one to be greater than half of the other ($MS_t \geq ½MS_g$; $MS_g \geq ½MS_g$). This was done by inverting the data, examining coefficients, adjusting multi-scattering limits if they did not meet this criteria, and re-running the inversion. While providing multi-scattering factors that appear reasonable for broadband considerations, there was no check to see if the optimally derived set of *eLAI* and $R_{x_n}$ would reasonably result in the derived $R_{zx_n}$ values. When inverting hyperspectral data, this process becomes computationally expensive. Empirical expressions for the multi-scattering factors were thus determined using a two-stream model of canopy radiative transfer [8]. Now as the inversion iterates over potential values of *eLAI*, resulting $R_x$ are used to determine multi-scattering factor limits based on this two-stream approximation as a function of spectral band. If any derived multi-scattering factors are outside these limits then the limits are applied and the inversion repeated.

## IV. Application

As partial validation, the multi-band FLAIR inversion model (mFLAIR) was run using the 2-band boreal forest data initially used to validate the single band FLAIR [11][14]. With multi-band inversion, one *eLAI* value is determined as optimal. It was found that the *eLAI* value determined with mFLAIR was always closest (within 0.25) of that derived for the near-infrared single band inversion, as expected [11]. Optimal sunlit $R_x$ values were usually smaller than their single band derived counterparts (< 20%) as were $MS_x$ (resulting in slightly larger values of $R_{zx}$).

Testing of this model is presently being performed on the Clinton agriculture hyperspectral imagery. This will

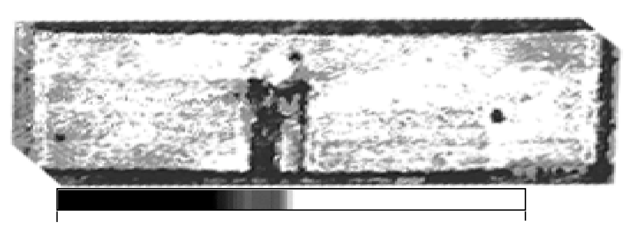


Fig. 1. Change in Equivalent Water Thickness (ΔEWT) when using the Water Index relation derived for pass-A on pass-B BRF data for the Pigbarn corn field. Mean ΔEWT = 0.011.

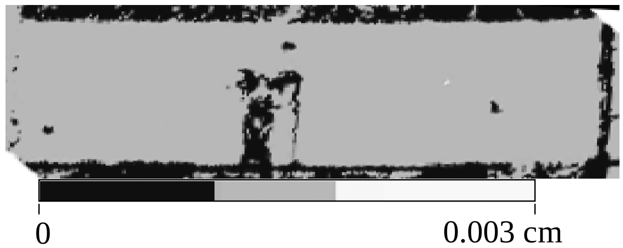


Fig. 2. Change in Equivalent Water Thickness (ΔEWT) when using the Water Index relation derived for pass-A on normalized pass-B BRF data for the Pigbarn corn field. Mean ΔEWT = 0.002.

investigate relationships between mFLAIR derived coefficients ($R_{x_n}$, *eLAI*) and field measurements. This study also considers the application of normalized data in developing VI – canopy characteristics relationships.

Using a corn field in the south-east corner of the study area (Pigbarn field) as an example preliminary study area, the effect of using mFLAIR to normalize canopy BRF before developing VI – canopy relationships is examined. Between flight lines (taken 45 minutes apart), the incident solar zenith angle changed from 43° (pass-A) to 35° (pass-B), with the result apparent as an increase in BRF. One study has previously developed an empirical relationship between the Water Index (WI = BRF(900nm) / BRF(970nm) [15]) and measured Equivalent Water Thickness (EWT) of corn using pass-A data [6]. When this relationship is applied to pass-B data, a decrease in derived EWT is noted, related only to the BRDF and not to any sudden change in field moisture. The difference in derived EWT using the pass-A WI – EWT relationship is demonstrated in Fig. 1.

By using the BRF values of this field from both passes, FLAIR inversion provides coefficients for this field which allows the BRF from pass-B to be normalized to pass-A solar geometry conditions. Once normalized, the developed WI – EWT relationship found to apply to pass-B (Fig. 2).

## V. Discussion – Conclusion

Preliminary study of normalizing observed BRF's of uniform crop canopies has demonstrated the potential of developing vegetation indices which are more generally applicable, and not limited to unique view/solar illumination geometries. Further work shall continue examine this potential for agricultural crops, other vegetative land cover classes, and various vegetation indices.

## References

[1] H. McNairn, J.C. Deguise, A. Pacheco, J. Shang, and N. Rabe, "Estimation of crop cover and chlorophyll from hyperspectral remote sensing", *Proc. 23rd Can. Symp. Remote Sensing*, Ste. Foy, PQ, 2001.

[2] P.J. Zarco-Tejada and J.R. Miller, "Land cover mapping at BOREAS using red edge spectral parameters from CASI imagery", *J. Geophy. Res.*, **104**(D22): 27921-27933, 1999.

[3] A. Pacheco, A. Bannari, J-C. Deguise, H. McNairn, and K. Staenz, "Application of hyperspectral remote sensing for LAI estimation in precision farming", *Proc. 23rd Can. Symp. Remote Sensing*, Ste. Foy, PQ, pp. 281-287, 2001.

[4] N.H. Broge and E. Leblanc "Comparing prediction power and stability of broadband and hyperspectral vegetation indices for estimation of green leaf area index and canopy chlorophyll density", *Remote Sens. Environ.*, **76**: 156-172, 2000.

[5] C. Champagne, A. Bannari, K. Staenz, J-C. Deguise, and H. McNairn, "Validation of a Hyperspectral Curve-Fitting Technique for Mapping Crop Water Status", *Proc. 23rd Can. Symp. Remote Sensing*, Ste. Foy, PQ, pp. 749-756, 2001.

[6] C. Champagne, *Remote Sensing of Plant Water Content for Precision Agriculture: The Potential for Hyperspectral Modelling*, MSc. Thesis, Graduate Program Geography, Univ. Ottawa, Ottawa, ON, 2002.

[7] K. Staenz, J-C. Deguise, J.M. Chen, H. McNairn, "Estimation of leaf area index (LAI) from crop fraction using hyperspectral data", submitted *ISPRS J. Photogrammetry and Remote Sensing*, 2001.

[8] P.J. Sellers, Vegetation-Canopy Spectral Reflectance and Biophysical Processes in *Theory and Applications of Optical Remote Sensing*., G. Asrar ed., John Whiley and Sons, New York, 1989, pp. 297-335.

[9] N.S. Goel, "Models of vegetative canopy reflectance and their use in estimation of biophysical parameters from reflectance data", *Remote Sens. Rev.*, **32**: 1-212, 1988.

[10] H.P. White, J.R. Miller, and J.M. Chen, "Four-scale linear model for anisotropic reflectance (FLAIR) for plant canopies. I: Model description and partial validation", *IEEE Trans. GeoSci. Remote Sens.*, **39**(5): 1072-1083, 2000.

[11] H.P. White, J.R. Miller, and J.M. Chen, "Four-scale linear model for anisotropic reflectance (FLAIR) for plant canopies. II: Partial validation and inversion using field measurements", accepted *IEEE Trans. GeoSci. Remote Sens.*, 2001.

[12] W. Wanner, X. Li, and A. Strahler, "On the derivation of kernel-driven models of bidirectional reflectance", *J. Geophys. Res.*, **100**(D10): 21077-21089, 1995.

[13] K. Staenz, T. Szeredi, and J. Schwarz, "ISDAS – A system for processing/analyzing hyperspectral data", *J. Remote Sens.*, **24**(2): 99-113.

[14] H.P. White, S.G. Leblanc, J. Cihlar, and J. Chen, "Mapping biophysical parameters with modelled and inverted functions from directional satellite measurements", *Proc. 23rd Can. Symp. Remote Sensing*, Ste. Foy, PQ, 2001.

[15] J. Peñuelas, I. Filella, L. Serrano, and R. Savé, "The reflectance at the 950-970 region as an indicator of plant water status", *Int. J. Remote Sens.*, **17**(2): 373-382.